Waste Management 211 (2026) 115283

Contents lists available at ScienceDirect

Waste Management

journal homepage: www.elsevier.com/locate/wasman

Research Paper

Experimental and environmental impact of early-stage lithium recovery in lithium-ion battery recycling

Dominic Dittmer [a,*,1], Abdur-Rahman Ali [b,1], Mahya Nezhadfard [c], Neill Bartie [d], Fabian Diaz [a], Steffen Blömeke [b], Daniel Schröder [c], Christoph Herrmann [b], Bernd Friedrich [a]

[a] Institute IME Process Metallurgy and Metal Recycling, RWTH Aachen University, Aachen, Germany
[b] Institute of Machine Tools and Production Technology (IWF), Chair of Sustainable Manufacturing and Life Cycle Engineering, Technische Universität Braunschweig, Braunschweig, Germany
[c] Institute of Energy and Process Systems Engineering (InES), Technische Universität Braunschweig, Braunschweig, Germany
[d] Helmholtz-Zentrum Berlin für Materialien und Energie (HZB), Berlin, Germany

ARTICLE INFO

Keywords:
Life cycle assessment
Battery recycling
Hydrometallurgy
Process simulation
NMC cathode

ABSTRACT

In December 2019, the European Union announced the Green Deal as a growth strategy to ensure a resource-efficient and competitive economy. Based on this, in 2023 targets for battery recycling were formulated in a regulation. It is imperative to enhance both the recovery rate and the quality of the material to comply with this regulatory requirement. Two hydrometallurgical battery recycling processes for black mass from lithium-ion batteries with nickel manganese cobalt oxide 111 have been examined. The experimental investigation focuses on comparing early-stage lithium recovery (ESLR) process route, were lithium is leached in a first step with water from the black mass before acid leaching, with a reference route. Based on this analysis, an initial process simulation was developed in HSC SIM to generate data for life cycle assessment. Results show that the ESLR route increases lithium recovery to 61.9 % in experiments, with higher product quality. Simulation-based analysis showed a 5.7 % reduction in climate change impact per kg black mass treated compared to the reference route. Improved lithium recovery and quality reduced the climate impact of secondary lithium carbonate by 16 %, and by 37 % if wind power replaces grid electricity. Among sixteen impact categories evaluated, the ESLR route has lower impacts than the reference in thirteen categories.

1. Introduction

Driven by the debate on climate change in society, the general population is more aware about the consequences of global warming on the environment. People around the world are gradually shifting towards electric vehicles (EVs) to reduce carbon emissions of combustion engine cars, which accelerate climate change. (Alanazi, 2023; IEA, International Energy Agency, 2022; Muratori et al., 2021) In addition to the demand for EVs, the demand for electronic mobile devices has also risen steadily (Fleischmann et al., 2023; Laricchia, 2023). The use of lithium-ion batteries (LIBs) in devices and EVs increases the amount of raw materials used like lithium, nickel, cobalt, and manganese (Hu et al., 2021; Maisel et al., 2023; Xu et al., 2020). Due to potential raw material supply risks, geopolitical access challenges, and their economic importance, these elements are classified as strategic for Europe. Consequently, the recycling of end-of-life LIBs is becoming increasingly important and necessary. (European Commission, 2023; Graham et al., 2021; Miao et al., 2022). In addition, the European Union has drawn up regulations to enable sustainability and climate neutrality by 2050 (European Union, 2023). From a materials-and-process perspective, achieving these goals requires metallurgical infrastructures and designs that respect energy requirements and minimize inevitable losses across the system (Reuter et al., 2019). To make LIB recycling economically and environmentally feasible and support the scaling from laboratory scale to industrial scale, current research is primarily focused on questions related to improving material recoveries, purities, and reducing accompanying waste streams (Ma et al., 2025; Machala et al., 2025; Natarajan & Aravindan, 2018; Swain, 2017).

While there are various types of LIBs like lithium nickel manganese cobalt oxide (NMC, with variable composition ratio like 523, 622, and

* Corresponding author.
E-mail address: ddittmer@ime-aachen.de (D. Dittmer).
[1] These authors contributed equally to this work.

https://doi.org/10.1016/j.wasman.2025.115283
Received 8 October 2025; Received in revised form 28 November 2025; Accepted 6 December 2025
Available online 16 December 2025

111)(Davis & Demopoulos, 2023), lithium cobalt oxide (LCO), lithium manganese oxide (LMO), lithium nickel cobalt aluminum oxide (NCA), and lithium iron phosphate (LFP) (Baum et al., 2022; Davis & Demopoulos, 2023; Kresse et al., 2022; Wang et al., 2021), there are also different mechanical, pyrometallurgical, hydrometallurgical, and biological methods for battery recycling. In comparison, hydrometallurgy offers higher yields and purities with comparatively low energy demand (Cerrillo-Gonzalez et al., 2024). Hereinafter referred to as the reference route, a common LIB recycling process according to Wang and Friedrich consists of acid leaching, copper cementation, iron-aluminum precipitation, nickel–cobalt-manganese (NMC) precipitation and the corresponding filtration steps with a final lithium precipitation by adding sodium carbonate (Wang & Friedrich, 2015).

Compared to EU regulations, hydrometallurgical processes lacks in recovery rates and need to be modified. For this, there are several process modifications in hydrometallurgy. Li et al. used a similar approach, where the authors used water leaching to recover graphite, copper foil and lithium (Li et al., 2021). Flotation is also a popularly used approach in hydrometallurgy and was generally addressed in the review of Chang et al., where they highlight the advantages of flotation regarding wastewater treatment and mineral beneficiation (Chang et al., 2019). Ruismäki et al. focused on flotation as well and pointed out the recovery of graphite and valuable metals from battery scrap (Ruismäki et al., 2020). Another important method is the solvent extraction, which is used to extract target metals from pregnant leaching solutions, but can also be used for the recovery of electrolyte as described by Lei et al. (Lei et al., 2022). Zhang et al. also used flotation to recover lithium from waste water of a spent LIB recycling process (Zhang et al., 2020). An additional approach, which combined hydro-mechanical and pyrometallurgical recycling was examined by Holzer et al. (Holzer et al., 2023).

An additional problem are lithium losses, which occur in each process step of hydrometallurgical processes, which leads to a low overall lithium recovery rate and further lower purity of every filter cake (Liu et al., 2021; Peng et al., 2019). This problem can generally be mitigated by introducing a step of water leaching, bringing only lithium into the solution, while most of the other elements remain in the black mass (Träger & Friedrich, 2016). In later works, this step of leaching black mass with water prior acid leaching was called early-stage lithium recovery (ESLR) (Milicevic Neumann et al., 2024; Schwich et al., 2021). The advantage of ESLR is the improved recovery and purity of lithium. However, from an aspired industrial scale, the question of the environmental impact on the remaining process should be further investigated due to the increased demand of water by the ESLR route and its associated increase in energy demand due to evaporation (Liu et al., 2021; Schwich et al., 2021). Since lithium is a critical element and a key resource for industry in future (European Union, 2023), this paper focusses the improvement of lithium recovery by ESLR.

To date, several studies have focused on the technical feasibility of ESLR concepts within battery recycling, however, without having a focus on their environmental impacts (Friedrich & Schwich, 2021; Milicevic Neumann et al., 2024; Munchen et al., 2024). System-level simulation coupled with life cycle assessment (LCA) has been shown to quantify trade-offs in recycling flowsheets and guide designs that improve recovery while reducing wastes (Reuter et al., 2015). Several studies within the field of LCA have focused on evaluating the environmental impacts of different recycling studies (Ali et al., 2024a; Blömeke et al., 2022; Chen et al., 2023; Chen et al., 2025; Husmann et al., 2023). Domingues and de Souza provide a review of LCA studies focusing on LIB recycling Domingues and de Souza, 2024. In some studies, process simulation was also used to generate the required data for LCA and assessing environmental impacts of battery recycling processes (Ali et al., 2024; Perocillo et al., 2025). Some of these studies used simulation-based LCA for the hydrometallurgical black mass recycling with the goal of reducing the environmental impacts of battery recycling processes and improving the extraction of valuable metals (Perocillo et al., 2025; Rinne et al., 2024). However, none of these studies have directly compared ESLR-based processes with conventional hydrometallurgical routes, especially not with regard to the environmental impacts of the recovered secondary materials. To bridge this gap, this study experimentally investigates the influence of ESLR on lithium recovery and purity, applies thermodynamic process simulation in HSC Chemistry to provide life cycle inventory data, and performs an LCA to compare environmental impacts of both routes as well as the secondary materials they produce (Scheidema et al., 2016).

This study investigates two hydrometallurgical recycling routes for black mass from end-of-life NMC111 batteries, focusing on the role of ESLR. Laboratory experiments were conducted to compare lithium recovery and product purity between the conventional route without and the modified route with ESLR, while also monitoring the recovery of Ni, Co, and Mn. The experimental data were used to build process simulations in HSC Chemistry, which provided additional information on energy, water, and wastewater flows and enabled a life cycle assessment (LCA). The LCA compares the two routes from a gate-to-gate perspective, identifies hotspots in environmental impacts, and evaluates the consequences for secondary materials such as Li_2CO_3, $Ni(OH)_2$, and $Co(OH)_2$ relative to primary production. In this way, the study assesses both the technical and environmental trade-offs of integrating ESLR into industrial battery recycling.

2. Materials and methods

2.1. Experimental procedure

The starting material was NMC 111 discharged pouch cells, which were thermally treated by pyrolysis at an adjusted temperature of 650 °C (max. 614 °C reached) with a heating rate of 300 °C/h and for a holding time of 150 min. With the intention to prevent the cells from burning and to avoid a thermal runaway, the process was conducted under an inert nitrogen atmosphere with a flow rate of 14 L/min. After pyrolysis, the frames of the cells, consisting of Al, were removed. In the following mechanical pretreatment, the remaining material was shredded in a shredding mill (Pulverisette 25, Fritsch GmbH) with a gap width of 4 mm. The resulting material was sieved in a vibratory sieve shaker (AS 200 control, Retsch GmbH) for 10 min with an amplitude of 1.5. The material, which passed the sieve with a mesh size of 250 μm was taken for the further process and is henceforth called as black mass. The analysis of the material is shown in Table A1.

Fig. 1 illustrates the ESLR route. In this approach, Li, due to its higher solubility, selectively dissolves into water from the black mass, while other metals remain in the solid phase (Schwich et al., 2021). After 120 min of reaction at room temperature with a solid-to-liquid ratio of 1:20 (black mass: water), the suspension is filtered. The Li-rich filtrate can then be evaporated to obtain solid Li compounds. A key advantage of ESLR is that no sodium is introduced at this stage, which is relevant since Li and Na are difficult to separate due to their chemical similarity (Zhang et al., 2025). Additionally, precipitation with Na_2CO_3 by the solubility product is difficult due to the low Li concentration (Cheng et al., 2013). This process modification is hereafter referred to as ESLR, while the conventional procedure is termed the reference route.

For applying the reference route as presented by Wang and Friedrich, 67.5 g of black mass was leached in the first step in 750 mL of a 2 M sulfuric acid solution for 2 h at 80 °C (see Fig. 1) (Wang & Friedrich, 2015). Additionally, 37.5 mL hydrogen peroxide was added over time to reduce Co and oxidize Cu. After filtration, graphite was received in the solid phase while the liquid solution was taken for the Cu cementation. For this, 7.5 M NaOH was dripped in until a pH of 1.18 was achieved, measured by an electrode (pH Sensor InPro4260i/SG, Mettler-Toledo GmbH). After adjusting the temperature to 60 °C, 5.85 g of Cu was added in the form of $CuSO_4$ to guarantee a filter cake for analysis after cementation. Additionally, 6.6 g Fe powder was inserted to enable the Cu cementation using an 1.25 overstoichiometric ratio and the reaction took place for 30 min, followed by a further filtration. In the next

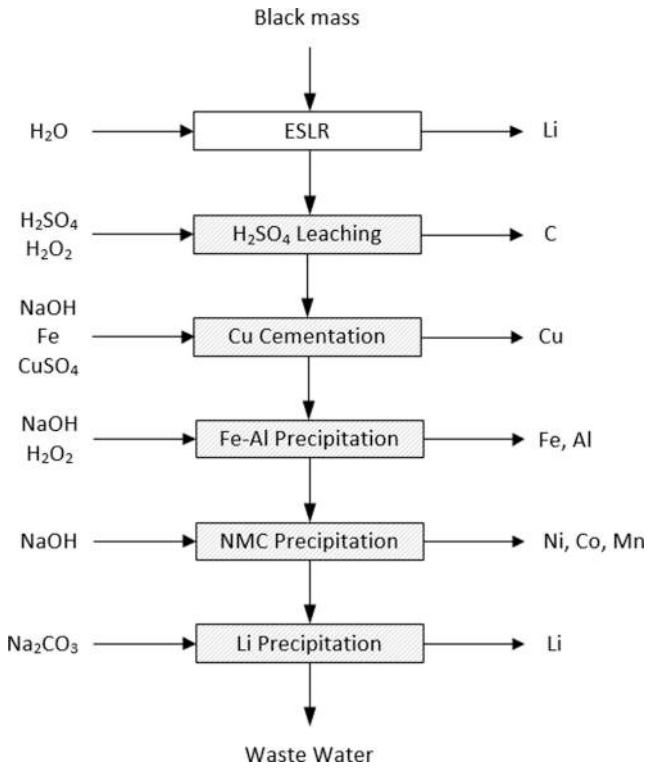

Fig. 1. Grey part: hydrometallurgical battery recycling process according to Wang and Friedrich (reference route); each step includes a filtration step (Wang and Friedrich, 2015); white part: process optimization.

step, the pH value of the cementation filtrate was raised to 2.6 by pipetting more NaOH at 60 °C. Then, 10 mL hydrogen peroxide was added to oxidize Fe^{2+} to Fe^{3+} completely. Due to this, the following pH increase with NaOH to 3.8 caused Al^{3+} and Fe^{3+} ions to precipitate, while Fe^{2+} would not have precipitated at this point. After a reaction time of 30 min, the suspension was filtrated to generate the Fe-Al filter cake and the filtrate for the NMC precipitation step. This was achieved by raising the pH value with NaOH to 10.4 at room temperature. After filtration, the last step was the Li_2CO_3 precipitation. For this, the previous filtrate was boiled down to 200 mL liquid. Then 75 mL of 150 g/L Na_2CO_3 was poured in at 95 °C. After 10 min of reaction, the solution was filtered to obtain precipitated Li_2CO_3. To evaluate the effectiveness of ESLR, each experiment was conducted twice using the same pyrolyzed black mass and following the methodology described above.

After every filtration, filter cakes were dried, crushed to below a particle size of 90 μm and homogenized, and a sample was taken of this as well as of the filtrate. The samples were analyzed by Inductively Coupled Plasma Optical Emission Spectrometry (ICP OES) for the elements Al, Cu, Co, Li, Mn, Ni, Fe, C and F. The following formula was used to calculate the elemental recoveries:

$$R = \frac{m_{element\_FC}}{m_{element\_input}}$$

In this formula $m_{element\_FC}$ is the mass of the specific element in the filter cake of the specific process and $m_{element\_input}$ the mass of the specific element entering the process. $m_{element\_input}$ consists of the amount of the specific element in the black mass and in case of Cu, Fe, and C additionally of the added mass in the different process steps.

2.2. Process simulation

The HSC Sim module of the HSC Chemistry software was used to generate the process-specific data needed to evaluate material recovery rates and to generate the data needed for environmental impact assessment of the reference and ESLR routes for the hydrometallurgical treatment of black mass. The required data for modeling the reference route was mostly taken from our experiments, and the proposed approach by Wang and Friedrich (Wang & Friedrich, 2015). Additionally, a process consisting of a sulfuric acid leach followed by oxidative precipitation proposed by Ichlas and colleagues was added to separate the mixed Ni, Co, and Mn hydroxides (Ichlas et al., 2020). Consumption of the chosen oxidant, ozone, was controlled so as to achieve the precipitation rates reported by the authors. The leaching and filtration process units for the ESLR route have been simulated according the aforementioned experiments. The simulated process was scaled up to be able to study the potential environmental impacts of a commercial scale battery recycling unit. The input to the hydrometallurgical treatment process was considered to be 60.94 kg black mass resulting from the mechanical treatment of one NMC111 battery pack. The process flowsheet created in HSC Sim is illustrated in Fig. 2. Note that the Ni, Co, and Mn hydroxide purification process is not shown. As depicted, the main difference between the reference and the ESLR routes is whether the black mass is treated in the neutral leach first (ESLR) or whether it goes directly to the acidic leach (reference). The results of the simulation models have then been converted into life cycle inventory (LCI) data, which were then coupled using an Excel interface to perform the life cycle impact assessment.

Chemical reactions considered in the simulations for modeling the acid leaching behavior of the black mass are provided in the Appendix. The leaching system involves H_2SO_4 as the primary leaching agent and H_2O_2 as an oxidizing agent. To ensure sufficient reagents for the reactions, the amount of H_2O_2 and H_2SO_4 used in the simulation was set higher than their calculated theoretical amounts, with an excess of 4 % and 16 %, respectively. The volume of H_2SO_4 needed was then used as the control parameter in the model to achieve the required pH value of 0.5. Another important parameter for the leaching process was the liquid-to-solid mass ratio (L/S ratio) which was set to 50 L/kg for this simulation based on the LithoRec process (Krüger et al., 2014; Kwade & Diekmann, 2018). A subsequent solid–liquid separation step via filtration was then added after leaching to remove potential undissolved metals and mainly graphite from leach liquor. A washing sequence has also been added to remove any residual leachate. Since leach liquor may still contain some impurities, i.e., Cu, Al or Fe, cementation has been considered for removing Cu impurities through the addition of Fe powder at 60 °C. For the selective precipitation process of cathode materials, i.e., Ni, Mn and Co from the final filtrate, the amount of NaOH was gradually increased to adjust the pH value of the solution at 25 °C. They were precipitated into their metal hydroxide forms as $Ni(OH)_2$, $Co(OH)_2$, and $Mn(OH)_2$. Li in the black mass was recovered as Li_2CO_3 by adding Na_2CO_3 to the solution. Evaporative crystallization at 110 °C has been considered to remove the moisture from the recovered Li_2CO_3 powder.

2.3. Life cycle assessment

The goal of the LCA is to compare the two hydrometallurgical process routes described above. The results of the LCA will identify hotspots and estimate the climate change impacts of the secondary materials recovered. The functional unit refers to the processing of 1 kg of NMC111 black mass. The input is considered burden free (i.e., without environmental impacts). Although upstream burdens (mechanical pretreatment, discharge, pyrolysis, and transport) would increase impacts proportionally for both routes without altering their relative ranking, the system boundary was deliberately restricted to the gate-to-gate hydrometallurgical stages to focus on the comparative performance of the two recycling routes.

The decision context of the study is “micro-level decision support,” therefore it is classified as Situation A (ILCD, 2010). Given this decision context, resource and energy use, along with related emissions from

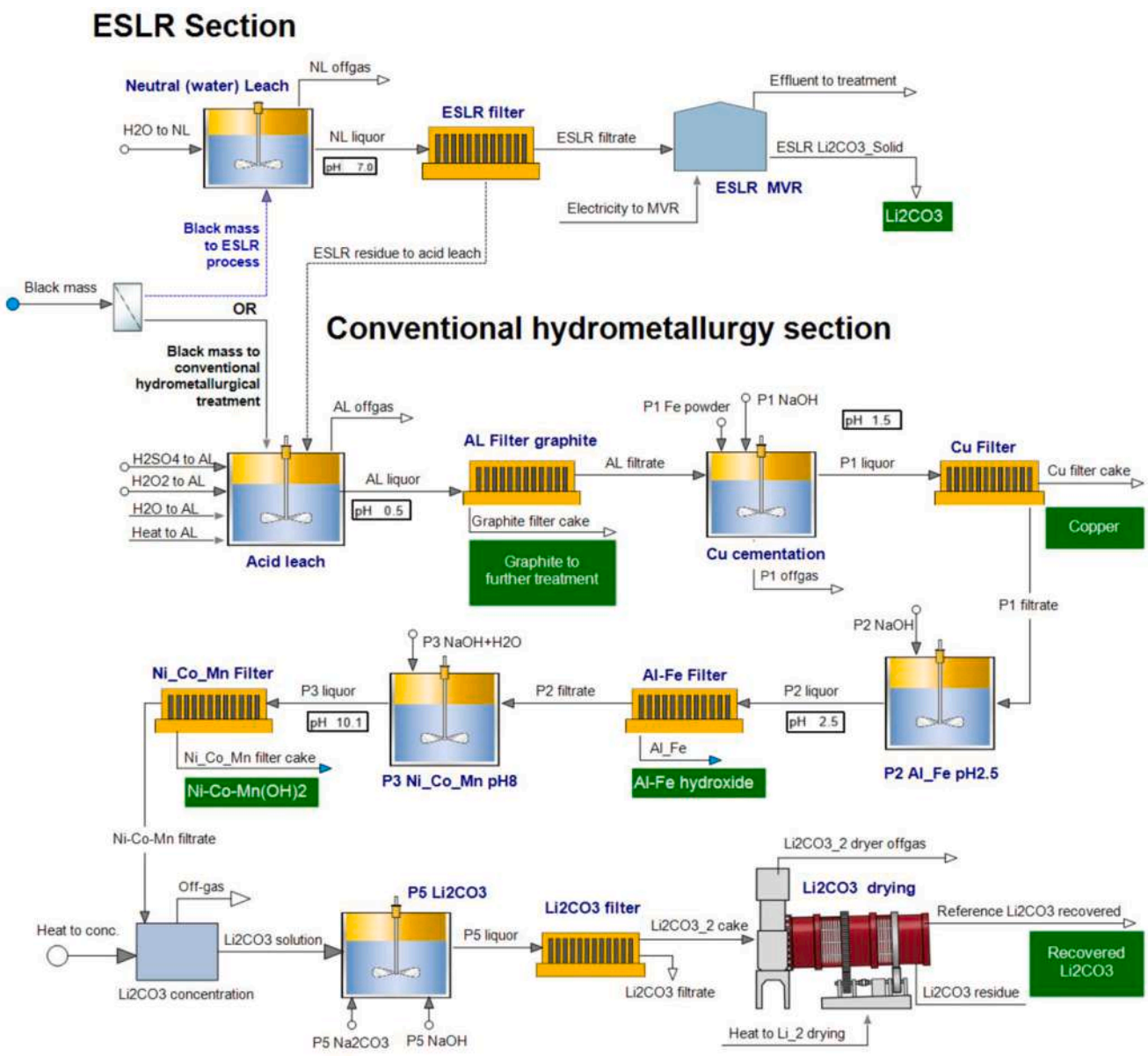

Fig. 2. The process flowsheet from HSC Sim for hydrometallurgical treatment with and without ESLR.

black mass treatment, were analyzed using an attributional modeling approach. The modeling of the background system is based on using average processes as indicated in the supplementary information (SI). The background system was modelled based on the ecoinvent 3.11 cut-off system model (Wernet et al., 2016). The black mass is considered to enter the system free of any burdens from any prior mechanical treatment. The LCA was performed using the activity browser software (Steubing et al., 2020). The impact assessment method used in the study is EF v3.1 (Andreasi Bassi et al., 2023). All sixteen impact categories in EF v3.1 are considered in the study to avoid problem-shifting across impact categories in the development of future process technologies. The results section highlights climate change and estimates secondary impacts of recovered battery materials. However, the results of all impact categories are reported and are available for further analysis in the SI. The secondary material impacts are derived based on a combination of mass and economic metrics (Ali et al., 2024; Husmann et al., 2023). The secondary material impacts in this study mean the potential environmental impacts of the materials recovered from recycling. This choice was selected as the economic value of the material recovered vary by more than a factor of 1000 (GBA, 2024). The 10-yr average metal prices were used for economic value and the details are provided in the SI (GBA, 2024).

The treatment of black mass occurs in Germany, and the treatment facility is assumed to process approximately 60.94 kg black mass per hour, i.e., chosen to represent one battery pack with NCM 111 cell chemistry per hour. The material flows of the hydrometallurgy treatment process are estimated based on the process simulations described above and the predicted recovery rates are compared with the experimental findings obtained in this study. The energy demand of individual unit processes in the hydrometallurgical treatment was estimated using empirical calculations and equipment supplier datasheets.

3. Results and discussion

This section shows the results of the hydrometallurgical battery recycling processes in form of the recoveries of the different elements including mass balances as well as the simulation based on it and the subsequent estimated environmental impacts.

3.1. Experimental results

Looking at the compositions of the filter cakes, large differences between the process steps can be observed (see Table A2). The filter cake after leaching contained mainly graphite (81.9 %), which is insoluble in H_2SO_4 (see Fig. A1.A). In contrast, the copper cementation step produced a filter cake with 79.5 % purity, reflecting the good selectivity of the process. Both filter cakes had high purity, with almost no other elements detected (< 0.2 %), except for 3.0 % Al in the leaching cake. The hydroxide filter cake after Fe–Al precipitation showed notable contaminations, including Co (1.0 %), Li (0.3 %), Mn (1.0 %), and Ni (1.2 %). A similar effect appeared after NMC precipitation, where the filter cake contained impurities such as Li (0.5 %) and Fe (0.5 %).The distribution of Ni, Co, Mn, and Li across the entire process can be seen in Fig. 3 comparing the process with and without ESLR. Fig. 3.A shows that nearly no Ni (< 0.3 %) left the process in ESLR, acid leaching and Cu cementation in both cases. This changed in Fe-Al precipitation. While in the route without ESLR 6.5 ± 0.2 % Ni precipitated, it was only 1.2 ± 0.2 % in the route with ESLR. A reason for this can be that experiments were conducted in too small scale. The main amount of Ni precipitated as expected in both routes in NMC precipitation. Without previously done ESLR, 92.4 ± 2.7 % Ni could be recovered here. In case with ESLR, this amount was reduced to 79.3 ± 9.5 %. Li precipitation resulted in less than 0.3 % Ni in both routes which simultaneously implies that there is only a small balance in the route without ESLR (1.2 ± 1.8 %), while the route with ESLR had a high balance of around 19.2 ± 9.6 %. Even though there is an additional process step with ESLR, the balance must have further reasons like errors in measurement, inhomogeneity in samples or inaccuracy in chemical analysis. The size of the error bars support this assumption. Co (Fig. 3.B) and Mn (Fig. 3.C) display similar distributions. The process steps ESLR, acid leaching, and Cu cementation resulted in amounts below 0.3 % for both routes. Also Li precipitation was insignificant with less than 0.3 % (Co) and 0.7 % (Mn). Fe-Al precipitation showed for Co and Mn more precipitated amount in the route without ESLR (5.6 ± 0.3 %, 5.6 ± 0.2 %) than in the route with ESLR (1.3 ± 0.2 %, 1.2 ± 0.1 %). NMC precipitation showed the biggest

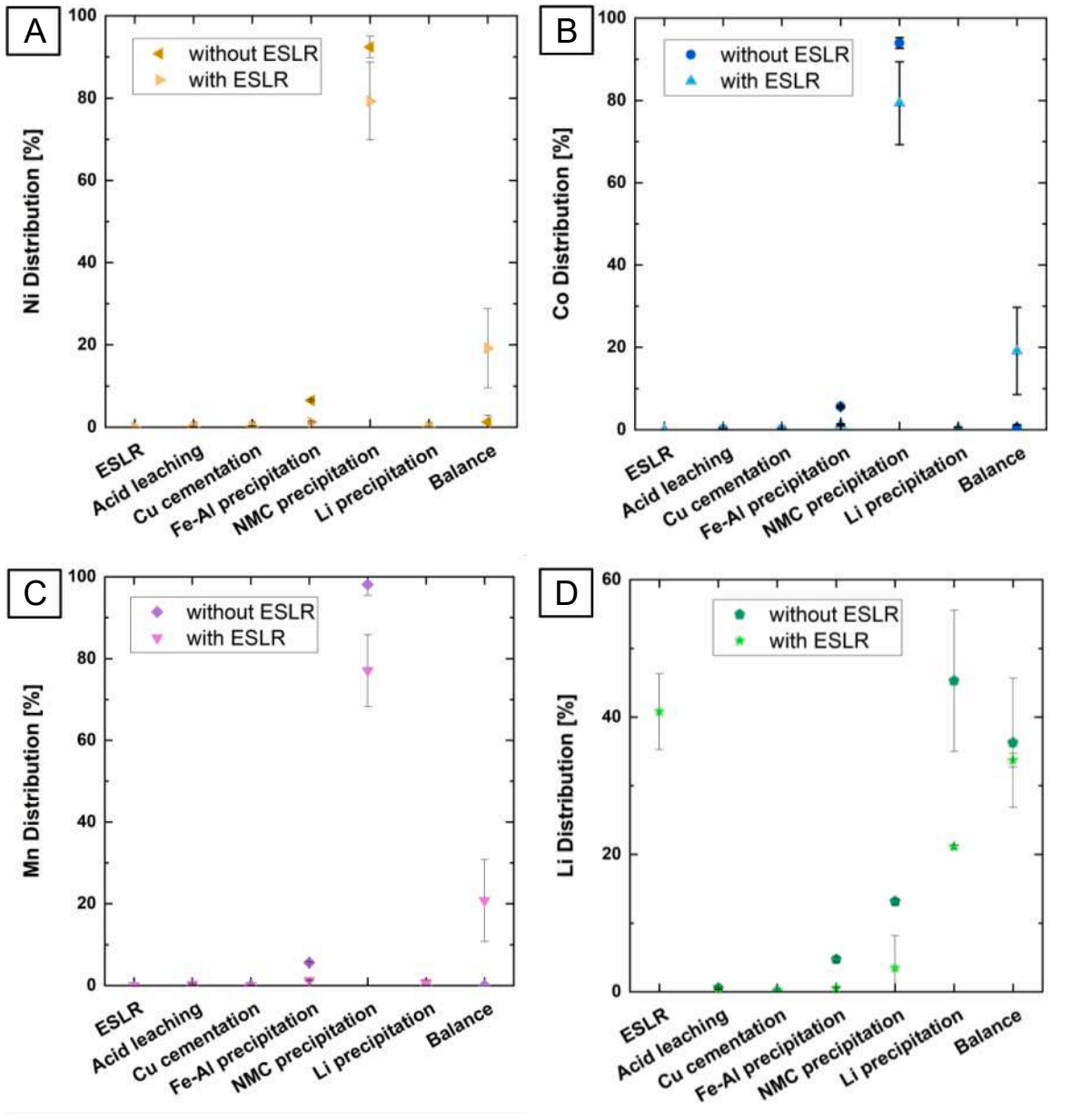

Fig. 3. Comparison of the elemental distribution in the routes with and without ESLR for A: Ni, B: Co, C: Mn, and D: Li.

differences here as well. Co and Mn precipitated mainly in this step in both cases but significantly more in the route without ESLR (94.0 ± 1.3 %, 98.1 ± 2.6 %) than with ESLR (79.3 ± 10.1 %, 77.1 ± 8.8 %). Similarly, the balances remained in the route without ESLR less than 0.5 % for both elements and were high (19.1 ± 10.6 %, 20.8 ± 10.0 %) with ESLR included. Since the behavior of Ni, Co, and Mn is very similar in general, the high balance can also be explained in the same way.

Fig. 3D shows the distribution of the route without and with ESLR for Li. The new process step allowed the recovery of 40.8 ± 5.5 % of the initial Li. Table A4 shows that the purity increased to 17.6 % Li compared to Li of the last step of the reference route. The filter cake contained 0.41 % Al and 11.5 % C. This leads to the hypothetical assumption that Li phases are mainly available as Li_2CO_3 and small amounts of $LiAlO_2$. In addition, phases such as Li_2O and LiF are probable. The acid leaching and Cu cementation steps showed the same results as aforementioned (see Fig. 3.D). The amount of Li in these filter cakes was negligible (< 0.6 %, < 0.1 %). The Fe-Al precipitation had a reduced amount of Li, decreasing from 4.7 ± 0.4 % in the reference route to 0.6 ± 0.0 % in the route with ESLR. The NMC precipitation revealed an even bigger decrease from 13.1 ± 0.4 % to 3.5 ± 4.7 %. The biggest difference is displayed for the Li treatment at the end of the process. While in the previous route 45.3 ± 10.3 % of the Li amount was recovered, in the route with ESLR only 21.1 ± 0.3 % was available, because a large amount of Li was already recovered in the ESLR process step. Due to the low purity in general in this process step because of the high amount of Na, it is an improvement to receive more Li in the ESLR process step. Regarding the total recovery and purity of Li products, the ESLR route is preferable. Nevertheless, the balances were nearly equally high in both cases with 36.3 ± 9.4 % in the reference route and 33.7 ± 1.0 % in the route with ESLR.

3.2. Recovery rates of battery active materials estimated by the HSC models

Table 1 shows the recoveries of Li, Co, Mn, and Ni as Li_2CO_3, Co$(OH)_2$, Mn$(OH)_2$ and Ni$(OH)_2$, respectively for the reference and ESLR processes as determined experimentally and via simulation. For comparison, literature values are also shown for each process route.

Comparing the reference and ESLR routes, experimental results show considerably increased Li recovery and decreased recoveries for Ni, Co, and Mn in the ESLR route. The decreased Ni, Co, and Mn recoveries are unexpected, as the ESLR process should only impact the distribution of Li through the process chain. Since more recent experimental work by one of the authors (Dittmer et al., 2025) where additional filter cake washing was investigated, show better alignment with expectations and simulation results, it is likely that experimental conditions or inaccuracies led to an underestimation of recoveries. In line with expectations for the ESLR route, simulation results also show significantly increased Li recovery. However, simulated Ni, Co, and Mn recoveries are only slightly lower compared to the reference and in line with more recent work mentioned above.

Within ESLR route results, simulated recoveries are considerably higher than those achieved in the experimental work. In absolute terms, simulated Li recovery is 30 % higher than the 61.9 % experimental value. Apart from inevitable experimental inaccuracies, a possible reason for this finding is the presence of water-insoluble Li compounds in the black mass as these cannot be recovered in the ESLR process. In the simulation, it is assumed that the only other Li compound present in the black mass following upstream pyrolysis is a small amount of lithium fluoride (LiF), which exhibits very limited water solubility. If others are present but not included in the simulation, simulated Li recoveries would be inflated. This is supported by the fact that more recent work (Dittmer et al., 2025) showed a 19 % higher experimental Li recovery - still below the simulated recovery of 92.5 % - while simulated Ni, Co, and Mn recoveries are in reasonable agreement (see Table 1). Although it is a separate and complex field of research, it is highly likely that some species in the black mass degrade into other, not yet fully understood phases during pyrolysis (Stallmeister & Friedrich, 2023; Stallmeister et al., 2025). Detailed mineralogical analysis of post-pyrolysis black mass would be a good starting point for this aspect of the simulation models to be refined.

Within reference route results, the simulated Li recovery is 15 % higher than the experimental result, while Ni, Co, and Mn recoveries are all within 3 % (relative) of one another. As was explained above regarding water solubility in ESLR, it is possible that Li species that exhibit low acid leach yields are present in the pyrolyzed black mass entering the processes investigated in this study. If such species are not captured in the model, simulated Li recoveries would be inflated. All recoveries, experimental and simulated, are in good agreement with the ranges reported by Wang and Friedrich (Wang & Friedrich, 2015). Even if recovered materials needed further processing to achieve the required precursor purity of more than 99 %, e.g. via solvent extraction (Petzold et al., 2025), the two process routes achieve policy-stipulated recovery rates for 2027 and 2031 were achieved (European Union, 2023; Kresse et al., 2022).

3.3. Environmental impacts of recycling routes

3.3.1. The life cycle inventory for treatment of 1 kg black mass

The outcome of the process simulation is the life cycle inventory for the two routes. An overview of the inventory is provided in Table 2. Both routes are normalized to one kilogram of black mass input. In terms of material demand, the sulfuric acid demand in the ESLR route is 9 % lower than the reference route. This is due to having an additional neutral leaching step in ESLR route, wherein the black mass is treated with water. This step decreases the quantity of black mass by separating Li before the next acid leaching process. However, this increases the water demand in the ESLR route and further need for its removal and treatment. The deionized water and electricity demand increased by nearly two and nine times compared to the reference route. Due to the ESLR, there is no demand for Na_2CO_3, as the lithium recovery steps in the later stage of the processes are removed compared to the reference route.

In terms of the by-products, the amount of Li_2CO_3 recovered in the ESLR has increased by 76 %. The quality of the Li_2CO_3 has also improved, as Li is recovered in the early stage of the process avoiding further material mixing and degradation. There are filter cakes that require further treatment. For instance, the graphite filter cake has about 87 % and 89 % graphite in the reference and ELSR route, respectively. Recovering graphite from filter cakes containing 80–90 % graphite is

Table 1
Comparison of experimental and simulated recoveries of Li, Co, Mn, and Ni in the Reference and ESLR routes.

	Reference route			ESLR route			EU Battery Regulation	
	Experi-mental	Simulated	(Wang and Friedrich, 2015)	Experi-mental	Simulated	Dittmer et al. (2025)	2027	2031
Li	45.3	52.2	48–64	61.9	92.5	81.2	≥ 50	≥ 80
Co	94.0	93.0	95–98	79.3	92.0	94.8	≥ 90	≥ 95
Mn	98.1	94.9	95–98	77.1	93.9	91.2	n/a	n/a
Ni	92.4	92.0	95–98	79.3	91.1	94.3	≥ 90	≥ 95

All recoveries in %. Note that the EU battery regulation does not specify targets for Mn as it is not a critical material.

Table 2
The aggregated life cycle inventory for the treatment of 1 kg of black mass from NMC111 battery pack via the reference route and the ESLR route. More details on the individual material streams and inventory data on a unit process level are available in SI.

Inputs			Output		
Name	Reference	ESLR	Name	Reference	ESLR
Materials (in kg)			**By-products (in kg)**		
Black mass	1.00	1.00	Nickel hydroxide	0.19	0.19
Sulfuric acid	1.62	1.48	Manganese hydroxide	0.17	0.17
Water (deionized)	25.78	48.94	Cobalt hydroxide	0.19	0.19
Hydrogen peroxide	0.15	0.15	Lithium carbonate	0.11	0.20
Sodium hydroxide	1.57	1.19	**Needs further treatment (in kg)**		
Sodium bicarbonate	0.32	0.00	Graphite filter cake	0.38	0.37
Ozone	0.16	0.15	Copper filter cake	0.01	0.01
Iron powder	0.01	0.01	Aluminum / iron filter cake	0.05	0.05
Treatment of wastewater	28.39	51.86			
Electricity & heat					
Electricity (in kWh)	0.20	1.71			
Heat (in MJ)	7.39	0.00			

technically feasible through combined physicochemical upgrading and thermal processing strategies. Filter cakes generated as by-products during hydrometallurgical battery recycling contain graphite and carbonaceous material suitable for anode recovery; upgrading can be achieved through thermal roasting at moderate temperatures (300–600 °C) combined with chemical leaching or flotation-based concentration to remove residual metal oxides, binders, and impurities (Wang et al., 2025); however, the environmental implications of such upgrading technologies must be evaluated using LCA models that compare the secondary impacts of recovered graphite against the avoided impacts of primary graphite production to determine overall process feasibility. However, the other filter cakes (such as Cu and Al-Fe) have low concentrations of metals and could not be viable toward further recycling. Under industrial conditions, such materials would typically be leached multiple times in a cascade configuration, which would result in a cleaner product but could also increase the environmental impact.

Table 3 shows product-specific electricity and heat demand for the reference and ESLR routes. Standard engineering correlations were used to estimate agitation and pumping power consumption (McCabe et al., 1967). Filter press power consumption was estimated from industrial specifications (Toper, 2025) and assumed cycle times. Evaporation duties based on enthalpy balances calculated in the model. However, due to the large volume of water to be removed in the ESLR process, a mechanical vapor recompression (MVR) system, based on a commercially available technology (Alfa, n.d.), was implemented to increase thermal efficiency.

Table 3
Product-specific electricity and heat consumption.

Electricity to drive equipment	**Reference**	**ESLR**	
ESLR neutral leach	–	0.101	kWh/kg Li_2CO_3
ESLR evaporation (MVR)	–	7.541	kWh/kg Li_2CO_3
Acid leach and graphite recovery	0.063	0.064	kWh/kg C
Cu cementation	2.233	2.141	kWh/kg Cu
Al- and Fe-hydroxide recovery	0.443	0.452	kWh/kg (Al, Fe)-hydroxides
Ni-, Co–, Mn-hydroxide recovery	0.039	0.040	kWh/kg (Ni, Co, Mn)-hydroxides
Li_2CO_3 precipitation	0.197	–	kWh/kg Li_2CO_3
Heat to drive evaporation	**Reference**	**ESLR**	
Li_2CO_3 concentration	61.8	–	MJ/kg Li_2CO_3
Final product drying	0.197	–	MJ/kg Li_2CO_3

In comparison to the reference route, the ESLR has a decreased material demand for chemicals such as sulfuric acid, sodium hydroxide, and sodium bicarbonate in addition to an increased electricity demand. This shift in material and energy demand needs to be considered based on their associated environmental impacts. In the next section, the environmental impacts of both routes and especially the secondary impacts of materials recovered are provided.

3.3.2. *Identification of environmental and secondary material impacts*

The contribution classified based of material, electricity, and heat toward the climate change impacts for the reference and ESLR route is depicted in Fig. 4 A. The materials contribute to about 84.8 % and 73.8 % of the total climate change impacts in reference and ESLR route, respectively. Within the materials, NaOH and ozone have the largest contribution. The additional electricity demand in the ESLR route for evaporation has increased its contribution to the ESLR route. In summary, the ESLR route has a 5.7 % lower climate change impact per kg black mass treated compared to the reference route.

In addition to having a lower climate change impact than the reference route, the ESLR route recovers 84.2 % more Li. This high recovery rate combined with the lower environmental impacts reduce the subsequent estimated impacts of secondary materials recovered as shown in Fig. 4 B. The secondary climate change impacts per kilogram material recovered is lower for all materials in the ESLR route. The secondary impacts of $Co(OH)_2$, Li_2CO_3 and $Ni(OH)_2$ are lower by 16 %, 16 %, and 14 % respectively. Furthermore, the allocation metrics shown in Fig. 4 B indicate an increased share of the recycling impacts being allocated to Li_2CO_3 in the ESLR route because of the increased material recovery. Finally, $Mn(OH)_2$ has a negligible impact due to its low market value in comparison to the other materials.

When interpreting the other impacts beyond climate change (see SI), the reference route has a higher impact than the ESLR route in thirteen out of the sixteen impact categories considered (see SI; Excel sheet "LCIA comparison"). Notably the ESLR route has a 11 % lower water use impact despite the increased demand in the inventory data as seen in Table 2. This trend can be attributed to the lower water use from material demand, especially Na_2CO_3. The largest difference in impacts between the two routes was seen in freshwater ecotoxicity and freshwater eutrophication. In the former, the ESLR route has a 28 % lower impact than the reference route, whereas in the latter, the impact was 31 % higher. The major contributor toward freshwater ecotoxicity is the chloride emission to surface water, and this is lower in the ESLR route due to the lack of Na_2CO_3 demand (see SI; Excel sheet "LCI comparison"). The phosphate emission to groundwater is responsible for majority of the freshwater eutrophication impacts. The reduction in material impacts in ELSR route is not in proportion to the increase in freshwater eutrophication impact due to increased electricity demand. In both impact categories, the material has a greater than 90 % contribution toward total impacts. Further analysis of the other impact categories is provided in the SI.

Furthermore, the climate change impact of the reference and ESLR route at 3.52 and 3.58 kg CO_2-eq/kg black mass treated is comparable with existing studies that provide disintegrated information on the level of black mass treatment. However, a direct comparison of any study is challenging due to the underlying variations in process technology, material recovery rates, and background datasets used in modelling. Rinne et al. (2024) reported climate change impact values between 5.44 and 7.96 kg CO_2-eq/kg black mass treated. Ali et al. (2024) reported climate change impact of 2.84 kg CO_2-eq/kg black mass treated. Hanna et al. reported climate change impacts between 2.54 and 2.95 kg CO_2-eq/kg battery pack (Hanna et al., 2025).

Although the ESLR route significantly enhances Li recovery, it also increases water use, wastewater generation, and electricity demand

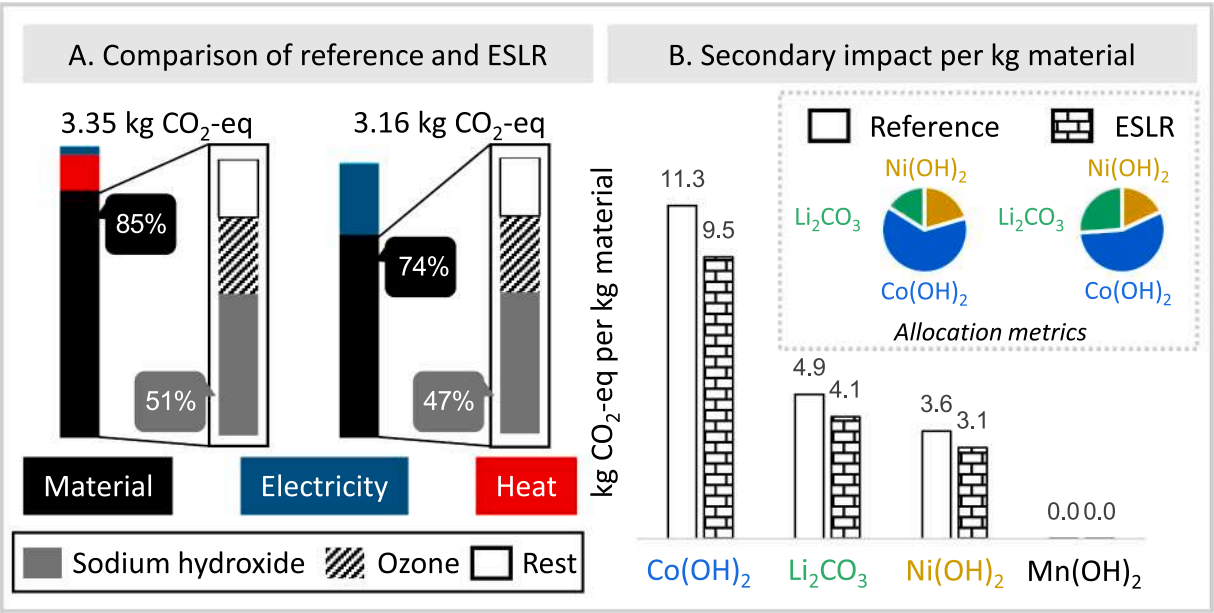

Fig. 4. A: The comparison of the climate change impacts between reference and the ESLR route based on the classification as material (further broken down), electricity, and rest; B: The secondary impact per kg of material recovered between the reference and the ESLR route along with the allocation metrics.

compared to the reference route. Multiple mitigation strategies can help address these challenges. First, implementing counter-current leaching or washing—well-known in hydrometallurgical setups - can improve reagent efficiency and reduce water and acid usage (Qadir et al., 2025). Second, recirculation the water recovered with mechanical vapor recompression (MVR) systems, can reduce water and wastewater treatment demand (Han et al., 2021; Si et al., 2021). Finally, optimizing the solid-to-liquid ratio during leaching, aiming for minimal dissolution volume while maximizing leach efficiency, is a common strategy to reduce water burdens especially when paired with effective washing steps that remove impurities without excess dilution. Together, these strategies present viable pathways to retain the recovery benefits of ESLR while improving further environmental performance.

3.3.3. *Role of secondary materials in meeting decarbonization goals*

The secondary materials recovered from battery recycling play a crucial role in achieving decarbonization goals of battery producers. This is primarily due to two reasons. The first being the regulatory landscape demanding increased use of secondary material in battery production and the second being the anticipated lower environmental impacts of secondary materials. The results, as shown in Fig. 4 B, indicate that the impacts of secondary materials can be lower than that of primary materials, especially for $Co(OH)_2$ and Li_2CO_3, where the primary impacts as indicated in ecoinvent 3.11 are around 33.2 and 7.7 kg CO_2-eq/kg of material (Wernet et al., 2016). However, there are instances where the impacts of primary Li production can be lower than 5.1 kg CO_2-eq/kg Li_2CO_3 (see Fig. 4 B), for instance Li_2CO_3 production via brines at Atacama (Schenker et al., 2022). The climate change impact values cited here are sourced from literature and the ecoinvent database, not direct industry data. Before drawing conclusions, note uncertainties and variabilities related to location, timing, and background assumptions like electricity mixes. It is also crucial to further reduce the environmental impacts of hydrometallurgical recycling, as these impacts are driven by the materials. For instance, producing ozone with renewable electricity rather than grid electricity in Europe. Sourcing key materials such as NaOH and O_3 with a lower impact than the reference values used via ecoinvent 3.11. Material substitution, such as replacing NaOH and ozone as an oxidant could also be envisaged as a potential strategy to further reduce impacts.

Since the Li recovery rates varied between the experiments and simulation, a sensitivity analysis on lower recovery rates of Li and its effect on impacts of the secondary materials was performed (see Excel sheet "ESLR (2)_experiment" in the SI). The analysis indicates reducing the Li recovery rate from 93.9 % to 61.9 % (keeping other material recovery rates the same as in values derived from simulation) still decreased the secondary Li_2CO_3 climate change impact by 5 % compared to reference route (see Excel sheet "Secondary impacts"). The water use impact increased by 10 % when lower recovery rates as in the experiments were factored in. This is observed as the reduction in the allocation factor towards lithium carbonate (from 0.26 to 0.18) due to lower lithium recovery was not commensurate to the lower lithium recovery. Furthermore, it was also investigated a scenario where the electricity is sourced from $>$ 3 MW onshore wind turbine, and it was found that the climate change and water use impact of recovered lithium carbonate decreases by nearly 11 % and 1 % respectively (see Excel sheet "ESLR (2)_electricity from wind" in the SI). Another scenario focused on the sourcing of ozone was considered. The ozone was sourced from locations outside Europe (Rest-of-World), and the results indicate that the climate change impact of recovered lithium carbonate increased by 30 % and water use impact reduced by 1 % (see Excel sheet "ESLR (2)_ozone from RoW" in the SI). Therefore, all scenarios considered expect sourcing of ozone still reduced the impacts of secondary materials compared to the reference. Any further reduction in climate change impacts of the recycling process such as by material substitution or sourcing will proportionally reduce the impacts of secondary materials. Therefore, trade-off between increased recovery yields at the cost of the environmental impacts need to be considered if the focus is on providing secondary materials with lower environmental impacts.

The importance of material supply chains on the overall environmental impacts of battery production is well demonstrated in literature. Ali et al. (2023) estimate that the choice of $NiSO_4$ production route alone could result in a 16 % difference in the climate change impacts of an NMC-based battery pack (Ali et al., 2023). Therefore, it is crucial to reduce the environmental impacts of battery recycling and improve the material recovery rates as this has a direct impact on the secondary material impacts.

Furthermore, it is worth nothing that the improvements indicated in this study are relative improvements, wherein two recycling routes and their secondary material impacts are compared. However, there are recent approaches to consider systems and products from an absolute

perspective, where the environmental impacts of different systems are compared against an environmental target rather than amongst themselves (Ali et al., 2024; Ali et al., 2025). In an absolute perspective, different recycling processes can be compared against an absolute target, wherein a target is set for the recycling process or on the environmental impacts of the secondary materials. Furthermore, the upscaling of the process can potentially decrease material and energy demands resulting in a lower carbon footprint of the materials.

4. Conclusion

This study compared a conventional hydrometallurgical recycling process for NMC111 black mass with a modified route including ESLR. Experimental results showed Li recovery of 45.3 % without ESLR and 61.9 % with ESLR, with a marked improvement in product purity from 4.3 % Li with high Na contamination to 17.6 % Li with negligible Na. Recovery rates for Ni, Co, and Mn were with more than 92 % high in the reference route and good with more than 77 % with ESLR, confirming that ESLR selectively enhances Li recovery with only small impact on other active materials, which is, however, attributable to the small scale in process execution.

Process simulations predicted higher Li recovery (93.9 %) than observed experimentally (61.9 %), highlighting uncertainties related to compound assumptions and phase transformations during pyrolysis. From an environmental standpoint, ESLR eliminated the need for sodium bicarbonate consumption; however, it required twice as much deionized water and wastewater treatment, as well as nine times more electricity. Despite this, the overall climate change impacts relative to the reference route was reduced by 5.7 %. Furthermore, when considering secondary material production, the ESLR route achieved lower climate change impacts per kilogram for all recovered product by 15 %. Overall, ESLR demonstrates a clear trade-off: higher resource and electricity demand versus significantly improved Li recovery, product quality, and lower secondary material impacts. Scenario analysis shows that sourcing electricity from wind can reduce climate change impacts of recovered lithium carbonate in ESLR by 36 % compared to the reference. At the same time, sourcing ozone outside Europe could increase the climate change impacts of recovered lithium carbonate by 9 % in comparison to reference. The ELSR route performed better than the reference in thirteen of the sixteen impact categories considered.

To enhance the industrial relevance of ESLR, future research should focus on optimizing washing strategies, implementing counter-current cascades, and improving solid–liquid ratios to reduce water demand and wastewater generation. Integration of energy-efficient evaporation technologies, such as mechanical vapor recompression, could offset the increased energy requirements. In addition, exploring material substitution for NaOH and ozone or adopting alternative purification methods may further reduce environmental impacts. Finally, scaling experiments under industrial conditions will be critical to validate laboratory findings and assess long-term operational feasibility. In a further step, the simulation can be used to predict process data for other black mass compositions.

CRediT authorship contribution statement

Dominic Dittmer: Writing – review & editing, Writing – original draft, Visualization, Validation, Resources, Methodology, Investigation, Formal analysis, Data curation, Conceptualization. **Abdur-Rahman Ali:** Writing – review & editing, Writing – original draft, Visualization, Software, Project administration, Methodology, Investigation, Formal analysis, Data curation, Conceptualization. **Mahya Nezhadfard:** Writing – review & editing, Writing – original draft, Visualization, Software, Methodology, Formal analysis, Conceptualization. **Neill Bartie:** Writing – review & editing, Validation, Software, Methodology, Formal analysis, Conceptualization. **Fabian Diaz:** Writing – review & editing, Supervision, Project administration, Methodology, Funding acquisition, Conceptualization. **Steffen Blömeke:** Writing – review & editing, Supervision, Project administration, Funding acquisition. **Daniel Schröder:** Writing – review & editing, Supervision, Funding acquisition. **Christoph Herrmann:** Writing – review & editing, Supervision, Funding acquisition. **Bernd Friedrich:** Writing – review & editing, Supervision, Funding acquisition.

Funding

The publication was funded by the German Federal Ministry of Education and Research under the Competence Cluster Recycling & Green Battery (greenBatt) for the project SIMTEGRAL, with grant numbers 03XP0331A and 03XP0331C.

Declaration of competing interest

The authors declare the following financial interests/personal relationships which may be considered as potential competing interests: All authors (corresponging and co-authors) reports financial support was provided by German Federal Ministry of Education and Research. If there are other authors, they declare that they have no known competing financial interests or personal relationships that could have appeared to influence the work reported in this paper.

Acknowledgment

The authors acknowledge all project partners for their support and feedback.

Appendix

Table A1
Composition of the used black mass.

Element	Al	Cu	Co	Li	Mn	Ni	Fe	C	F
wt%	3.19	0.05	8.18	3.44	7.70	8.24	0.00	4.21	3.99

Table A2
Mass of the filter cakes.

Process step	Leaching	Cu cementation	Fe-Al precipitation	NMC precipitation	Li precipitation
Mass of filter cake [g]	34.85	6.1	30.46	63.42	11.72

Table A3
Recoveries of the process.

	Al	Cu	Co	Li	Mn	Ni	Fe	C
Acid Leaching	49.20 %	0.00 %	0.10 %	0.47 %	0.09 %	0.10 %	0.00 %	96.13 %
Cu cementation	0.01 %	82.36 %	0.10 %	0.08 %	0.09 %	0.19 %	0.08 %	0.03 %
Fe-Al precipitation	11.60 %	0.34 %	5.41 %	4.46 %	5.80 %	6.41 %	103.84 %	0.03 %
NMC precipitation	0.00 %	0.68 %	94.87 %	12.84 %	96.27 %	94.30 %	4.61 %	0.36 %
Li precipitation	0.00 %	0.00 %	0.00 %	4.34 %	0.00 %	0.00 %	0.00 %	0.03 %
Li filtrate	0.14 %	0.00 %	0.00 %	48.20 %	0.01 %	0.05 %	0.00 %	0.00 %

Table A4
Composition of the ESLR product.

Element	**Al**	**Cu**	**Co**	**Li**	**Mn**	**Ni**	**Fe**	**C**
Components in ESLR filter cake [%]	0.41	0.001	0.0015	17.6	0.003	0.004	0.15	11.50

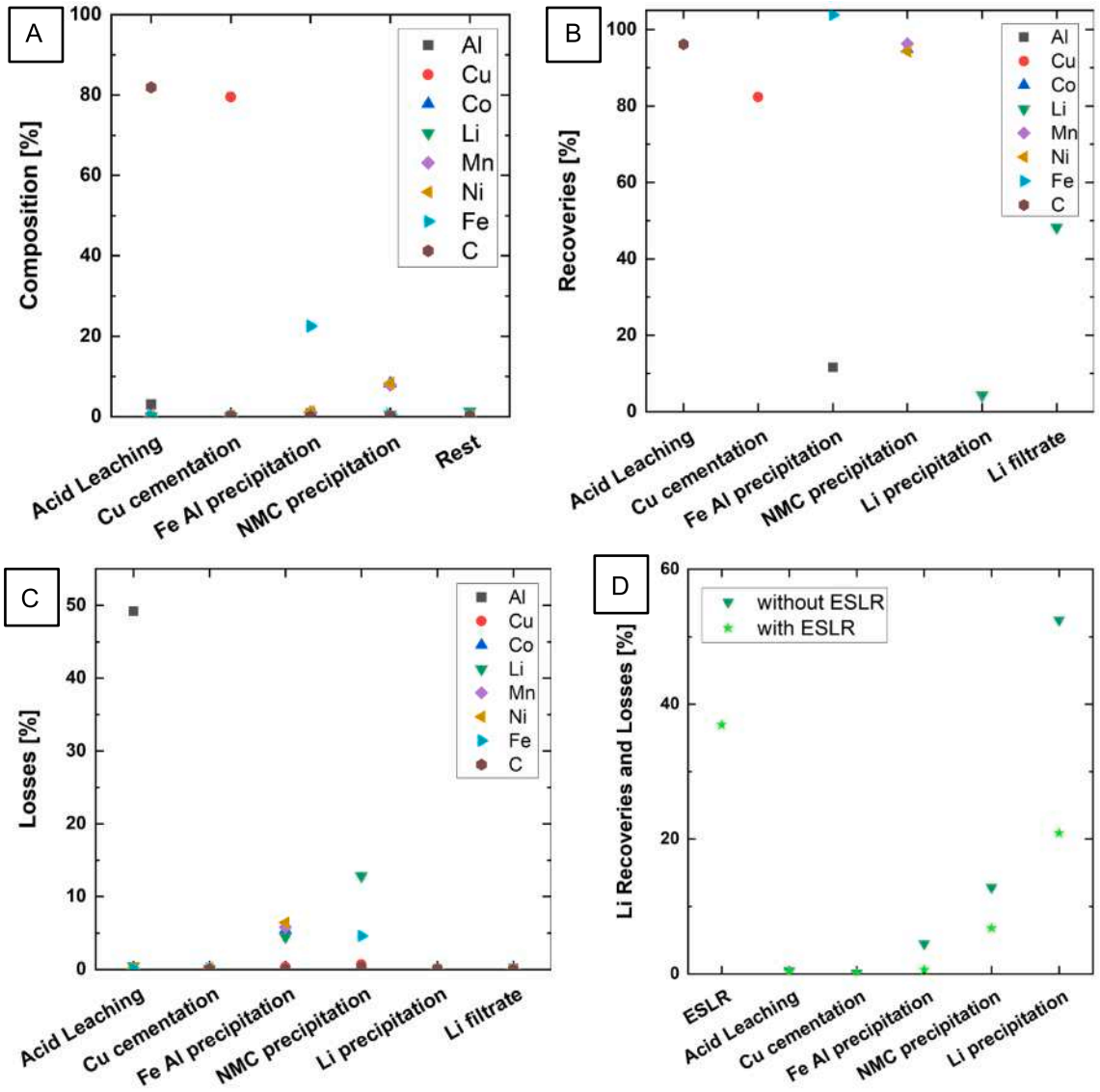

Fig. A1. A: Composition of filter cakes; B and C: recoveries and losses of the different elements in the different process steps of the recycling process; D: Comparison of Li recoveries of the recycling process without and with ESLR

Reactions considered in HSC simulations including the dissolution of various metal oxides and elemental metals commonly present in the black mass.

$$MnO + H_2SO_4\,(a) = MnSO_4\,(a) + H_2O \quad (1)$$

$$Mn_3O_4 + 3\,H_2SO_4\,(a) + H_2O_2\,(a) = 3\,MnSO_4\,(a) + 4\,H_2O + O_2\,(g) \quad (2)$$

$$Co + H_2SO_4\,(a) + H_2O_2\,(a) = CoSO_4\,(a) + 2\,H_2O \quad (3)$$

$$CoO + H_2SO_4\,(a) = Co\,(+2a) + H_2O + SO_4\,(-2a) \quad (4)$$

$$Ni + H_2SO_4\,(a) + H_2O_2\,(a) = NiSO_4\,(a) + 2\,H_2O \quad (5)$$

$$Li_2O + H_2SO_4(a) = Li_2SO_4(a) + H_2O \quad (6)$$

$$2\,LiF + H_2SO_4\,(a) = Li_2SO_4\,(a) + 2\,HF\,(a) \quad (7)$$

$$2\,Fe + 3\,H_2SO_4\,(a) + 3\,H_2O_2\,(a) = Fe_2\,(SO_4)_3 + 6\,H_2O \quad (8)$$

$$2\,Al + 3\,H_2SO_4\,(a) + 3\,H_2O_2\,(a) = Al_2\,(SO_4)_3(a) + 6\,H_2O \quad (9)$$

$$Al_2O_3 + 3\ H_2SO_4\ (a) = Al_2(SO_4)_3\ (a) + 3\ H_2O \quad (10)$$

$$Cu + H_2SO_4\ (a) + H_2O_2\ (a) = CuSO_4\ (a) + 2\ H_2O \quad (11)$$

Table A5
Chemical analysis of filter cakes of the experiments.

without ESLR	Experiment 1				Experiment 2			
	Co	Li	Mn	Ni	Co	Li	Mn	Ni
Acid leaching	0.10 %	0.47 %	0.09 %	0.10 %	0.15 %	0.62 %	0.13 %	0.16 %
Cu cementation	0.10 %	0.08 %	0.09 %	0.19 %	0.01 %	0.01 %	0.01 %	0.14 %
Fe-Al precipitation	5.41 %	4.46 %	5.80 %	6.41 %	5.80 %	4.99 %	5.46 %	6.64 %
NMC precipitation	94.87 %	12.84 %	96.27 %	94.30 %	93.07 %	13.43 %	99.99 %	90.56 %
Li precipitation	0.00 %	52.54 %	0.01 %	0.05 %	0.00 %	38.01 %	0.02 %	0.02 %
Balance	0.00 %	29.61 %	0.00 %	0.00 %	0.97 %	42.93 %	0.00 %	2.48 %
with ESLR	Experiment 3				Experiment 4			
	Co	Li	Mn	Ni	Co	Li	Mn	Ni
ESLR	0.00 %	36.91 %	0.00 %	0.00 %	0.00 %	44.71 %	0.00 %	0.00 %
Acid leaching	0.03 %	0.36 %	0.49 %	0.04 %	0.02 %	0.28 %	0.01 %	0.02 %
Cu cementation	0.00 %	0.00 %	0.00 %	0.17 %	0.00 %	0.00 %	0.00 %	0.30 %
Fe-Al precipitation	1.37 %	0.59 %	1.29 %	1.36 %	1.13 %	0.56 %	1.12 %	1.09 %
NMC precipitation	86.46 %	6.79 %	83.30 %	85.96 %	72.19 %	0.14 %	70.88 %	72.58 %
Li precipitation	0.50 %	20.90 %	1.17 %	0.09 %	0.04 %	21.31 %	0.12 %	0.03 %
Balance	11.63 %	34.45 %	13.75 %	12.37 %	26.61 %	33.01 %	27.87 %	25.98 %

Appendix A. Supplementary data

Supplementary data to this article can be found online at https://doi.org/10.1016/j.wasman.2025.115283.

Data availability

Data already shared in appendix and supplementary files.

References

Alanazi, F., 2023. Electric Vehicles: Benefits, Challenges, and Potential Solutions for Widespread Adaptation. Appl. Sci. 13 (10), 6016. https://doi.org/10.3390/app13106016.

Alfa, L. (n.d.). Alfa Laval AlfaFlash ZLD MVR systems. https://www.alfalaval.ae/globalassets/documents/products/process-solutions/evaporation-systems/alf0691_product_leaflet_korr02.pdf?utm_source=chatgpt.com.

Ali, A.-R., Bartie, N., Husmann, J., Cerdas, F., Schröder, D., Herrmann, C., 2024. Simulation-based life cycle assessment of secondary materials from recycling of lithium-ion batteries. Resour. Conserv. Recycl. 202, 107384. https://doi.org/10.1016/j.resconrec.2023.107384.

Ali, A.-R., Derin, D., Blömeke, S., Herrmann, C., 2025. Parametric life cycle assessment model for absolute environmental sustainability assessment of lithium-ion batteries. Sustainable Prod. Consumption 57, 80–94. https://doi.org/10.1016/j.spc.2025.05.010.

Ali, A.-R., Lackner, J., Cerdas, F., Herrmann, C., 2023. Analysis of nickel sulphate datasets used in lithium-ion batteries. Procedia CIRP 116, 348–353. https://doi.org/10.1016/j.procir.2023.02.059.

Andreasi Bassi, S., Biganzoli, F., Ferrara, N., Amadei, A., Valente, A., & Sala, S. (2023). Updated characterisation and normalisation factors for the environmental footprint 3.1 method (JRC technical report JRC130796). Europäische Kommission. https://op.europa.eu/en/publication-detail/-/publication/145f8401-a82a-11ed-b508-01aa75ed71a1 doi: 10.2760/798894.

Baum, Z.J., Bird, R.E., Yu, X., Ma, J., 2022. Lithium-Ion Battery Recycling—Overview of Techniques and Trends. ACS Energy Lett. 7 (2), 712–719. https://doi.org/10.1021/acsenergylett.1c02602.

Blömeke, S., Scheller, C., Cerdas, F., Thies, C., Hachenberger, R., Gonter, M., Herrmann, C., Spengler, T.S., 2022. Material and energy flow analysis for environmental and economic impact assessment of industrial recycling routes for lithium-ion traction batteries. J. Clean. Prod. 377, 134344. https://doi.org/10.1016/j.jclepro.2022.134344.

Cerrillo-Gonzalez, M., Villen-Guzman, M., Vereda-Alonso, C., Rodriguez-Maroto, J., Paz-Garcia, J., 2024. Towards Sustainable Lithium-Ion Battery Recycling: Advancements in Circular Hydrometallurgy. Processes 12 (7), 1485. https://doi.org/10.3390/pr12071485.

Chang, L., Cao, Y., Fan, G., Li, C., Peng, W., 2019. A review of the applications of ion floatation: Wastewater treatment, mineral beneficiation and hydrometallurgy. RSC Adv. 9 (35), 20226–20239. https://doi.org/10.1039/c9ra02905b.

Chen, Q., Hou, Y., Lai, X., Shen, K., Gu, H., Wang, Y., Guo, Y., Lu, L., Han, X., Zheng, Y., 2023. Evaluating environmental impacts of different hydrometallurgical recycling technologies of the retired nickel-manganese-cobalt batteries from electric vehicles in China. Sep. Purif. Technol. 311, 123277. https://doi.org/10.1016/j.seppur.2023.123277.

Chen, Q., Lai, X., Zhang, Y., Chen, J., Zhu, Z., Huang, Y., Zheng, Y., Song, X., Tang, B., Han, X., Lu, L., Ouyang, M., 2025. Environmental impacts and supply risks for LiFePO4 - LiCo Ni Mn O2 hybrid battery pack in China. Process Saf. Environ. Prot. 198, 107115. https://doi.org/10.1016/j.psep.2025.107115.

Cheng, W., Li, Z., Cheng, F., 2013. Solubility of Li2CO3 in Na–K–Li–Cl brines from 20 to 90 °C. J. Chem. Thermodyn. 67, 74–82. https://doi.org/10.1016/j.jct.2013.07.024.

Davis, K., Demopoulos, G.P., 2023. Hydrometallurgical recycling technologies for NMC Li-ion battery cathodes: current industrial practice and new R&D trends. RSC Sustainability 1 (8), 1932–1951. https://doi.org/10.1039/D3SU00142C.

Dittmer, D., Andary, M., Diaz, F., & Friedrich, B. (2025). Evaluation of filter cake washing processes in hydrometallurgical battery recycling of lithium-ion batteries to optimize recoveries.

Domingues, A.M., de Souza, R.G., 2024. Review of life cycle assessment on lithium-ion batteries (LIBs) recycling. Next Sustainability 3, 100032. https://doi.org/10.1016/j.nxsust.2024.100032.

European Commission. (2023). Critical raw materials. https://single-market-economy.ec.europa.eu/sectors/raw-materials/areas-specific-interest/critical-raw-materials_en?utm_source=chatgpt.com.

European Union (2023). Regulation (EU) 2023/ of the European Parliament and of the Council of July 12, 2023 concerning batteries and waste batteries, amending Directive 2008/98/EC and Regulation (EU) 2019/1020, and repealing Directive 2006/66/EC. https://eur-lex.europa.eu/legal-content/EN/TXT/PDF/?uri=CELEX:32023R1542.

Fleischmann, J., Hanicke, M., Horetsky, E., Ibrahim, D., Jautelat, S., Linder, M., Schaufuss, P., Torscht, L., & van de Rijt, A. (2023). battery-2030-resilient-sustainable-and-circular.

Friedrich, B., Schwich, L., 2021. New Science Based Concepts for Increased Efficiency in Battery Recycling. Metals 11 (4), 533. https://doi.org/10.3390/met11040533.

GBA (2024). Greenhouse Gas Rulebook Green Rules - Version 2.0.

Graham, J.D., Rupp, J.A., Brungard, E., 2021. Lithium in the Green Energy Transition: The Quest for Both Sustainability and Security. Sustainability 13 (20), 11274. https://doi.org/10.3390/su132011274.

Han, D., Chen, J., Zhou, T., Si, Z., 2021. Experimental investigation of a batched mechanical vapor recompression evaporation system. Appl. Therm. Eng. 192, 116940. https://doi.org/10.1016/j.applthermaleng.2021.116940.

Hanna, F., Somers, C., Anctil, A., 2025. Life Cycle Assessment of Lithium-Ion Battery Recycling: Evaluating the Impact of Recycling Methods and Location. Environ. Sci. Technol. 59 (28), 14432–14443. https://doi.org/10.1021/acs.est.4c13838.

Holzer, A., Zimmermann, J., Wiszniewski, L., Necke, T., Gatschlhofer, C., Öfner, W., Raupenstrauch, H., 2023. A Combined Hydro-Mechanical and Pyrometallurgical

Recycling Approach to Recover Valuable Metals from Lithium-Ion Batteries Avoiding Lithium Slagging. Batteries 9 (1), 15. https://doi.org/10.3390/batteries9010015.
Hu, S., He, S., Jiang, X., Wu, M., Wang, P., Li, L., 2021. Forecast and Suggestions on The Demand of Lithium, Cobalt, Nickel and Manganese Resources in China's New Energy Automobile Industry. IOP Conf. Ser.: Earth Environ. Sci 769 (4), 42018. https://doi.org/10.1088/1755-1315/769/4/042018.
Husmann, J., Ali, A.-R., Cerdas, F., Herrmann, C., 2023. The influence of stakeholder perspectives on the end-of-life allocation in the life cycle assessment of lithium-ion batteries. Front. Sustainability 4, 1163207. https://doi.org/10.3389/frsus.2023.1163207.
Ichlas, Z.T., Mubarok, M.Z., Magnalita, A., Vaughan, J., Sugiarto, A.T., 2020. Processing mixed nickel-cobalt hydroxide precipitate by sulfuric acid leaching followed by selective oxidative precipitation of cobalt and manganese. Hydrometall. 191, 105185. https://doi.org/10.1016/j.hydromet.2019.105185.
IEA, International Energy Agency (2022). Global Electric Vehicle Outlook 2022.
ILCD. (2010). General guide for Life Cycle Assessment: Provisions and action steps (First edition). Publications Office. doi: 10.2788/94987.
Kresse, Carolin, Bastian, Dennis, Bookhagen, Britta, Frenzel, & Max (2022). Lithium-Ionen-Batterierecycling in Deutschland und Europa.
Krüger, S., Hanisch, C., Kwade, A., Winter, M., Nowak, S., 2014. Effect of impurities caused by a recycling process on the electrochemical performance of Li [Ni0.33Co0.33Mn0.33]O2. J. Electroanal. Chem. 726, 91–96. https://doi.org/10.1016/j.jelechem.2014.05.017.
Kwade, A., Diekmann, J., 2018. Recycling of Lithium-Ion Batteries. Springer International Publishing. https://doi.org/10.1007/978-3-319-70572-9.
Laricchia, F. (2023). Forecast number of mobile devices worldwide from 2020 to 2025. https://www.statista.com/statistics/245501/multiple-mobile-device-ownership-worldwide/#statisticContainer.
Lei, S., Sun, W., Yang, Y., 2022. Solvent extraction for recycling of spent lithium-ion batteries. J. Hazard. Mater. 424 (Pt D), 127654. https://doi.org/10.1016/j.jhazmat.2021.127654.
Li, J., He, Y., Fu, Y., Xie, W., Feng, Y., Alejandro, K., 2021. Hydrometallurgical enhanced liberation and recovery of anode material from spent lithium-ion batteries. Waste Management (New York N.Y.) 126, 517–526. https://doi.org/10.1016/j.wasman.2021.03.052.
Liu, F., Peng, C., Ma, Q., Wang, J., Zhou, S., Chen, Z., Wilson, B.P., Lundström, M., 2021. Selective lithium recovery and integrated preparation of high-purity lithium hydroxide products from spent lithium-ion batteries. Sep. Purif. Technol. 259, 118181. https://doi.org/10.1016/j.seppur.2020.118181.
Ma, X., Meng, Z., Bellonia, M.V., Spangenberger, J., Harper, G., Gratz, E., Olivetti, E., Arsenault, R., Wang, Y., 2025. The evolution of lithium-ion battery recycling. Nature Reviews Clean Technology 1 (1), 75–94. https://doi.org/10.1038/s44359-024-00010-4.
Machala, M.L., Chen, X., Bunke, S.P., Forbes, G., Yegizbay, A., de Chalendar, J.A., Azevedo, I.L., Benson, S., Tarpeh, W.A., 2025. Life cycle comparison of industrial-scale lithium-ion battery recycling and mining supply chains. Nat. Commun. 16 (1), 988. https://doi.org/10.1038/s41467-025-56063-x.
Maisel, F., Neef, C., Marscheider-Weidemann, F., Nissen, N.F., 2023. A forecast on future raw material demand and recycling potential of lithium-ion batteries in electric vehicles. Resour. Conserv. Recycl. 192, 106920. https://doi.org/10.1016/j.resconrec.2023.106920.
McCabe, W. L., Smith, J. C., & Harriott, P. (1967). Unit operations of chemical engineering.
Miao, Y., Liu, L., Zhang, Y., Tan, Q., Li, J., 2022. An overview of global power lithium-ion batteries and associated critical metal recycling. J. Hazard. Mater. 425, 127900. https://doi.org/10.1016/j.jhazmat.2021.127900.
Milicevic Neumann, K., Ans, M., Friedrich, B., 2024. Early-stage recovery of lithium from spent batteries via CO2-assisted leaching optimized by response surface methodology. Sci. Rep. 14 (1), 17369. https://doi.org/10.1038/s41598-024-67761-9.
Munchen, D.D., Milicevic Neumann, K., Öner, I.E., Friedrich, B., 2024. Transfer of Early-Stage Lithium Recovery from Laboratory-Scale Water Leaching to Upscale Challenges. Metals 14 (1), 67. https://doi.org/10.3390/met14010067.
Muratori, M., Alexander, M., Arent, D., Bazilian, M., Cazzola, P., Dede, E.M., Farrell, J., Gearhart, C., Greene, D., Jenn, A., Keyser, M., Lipman, T., Narumanchi, S., Pesaran, A., Sioshansi, R., Suomalainen, E., Tal, G., Walkowicz, K., Ward, J., 2021. The rise of electric vehicles—2020 status and future expectations. Prog. Energy 3 (2), 22002. https://doi.org/10.1088/2516-1083/abe0ad.
Natarajan, S., Aravindan, V., 2018. Recycling Strategies for Spent Li-Ion Battery Mixed Cathodes. ACS Energy Lett. 3 (9), 2101–2103. https://doi.org/10.1021/acsenergylett.8b01233.
Peng, C., Liu, F., Wang, Z., Wilson, B.P., Lundström, M., 2019. Selective extraction of lithium (Li) and preparation of battery grade lithium carbonate (Li2CO3) from spent Li-ion batteries in nitrate system. J. Power Sources 415, 179–188. https://doi.org/10.1016/j.jpowsour.2019.01.072.
Perocillo, Y.K., Pirard, E., Léonard, A., 2025. Process simulation-based LCA: Li-ion battery recycling case study. The International Journal of Life Cycle Assessment. Advance online publication. https://doi.org/10.1007/s11367-025-02478-z.
Petzold, M., Büscher, D., Vrucak, D., Woeste, R., Hense, P., Flamme, S., Friedrich, B., Letmathe, P., 2025. A techno-economic evaluation of the hydrometallurgical recycling of mixed CAM black mass from spent LIB cells. Waste Management (New York N.Y.), 207, 115109. https://doi.org/10.1016/j.wasman.2025.115109.
Qadir, M.R., Bruckard, W.J., Chen, M., 2025. Countercurrent leaching of lithium-ion battery waste under ambient conditions. Miner. Eng. 234, 109703. https://doi.org/10.1016/j.mineng.2025.109703.
Reuter, M.A., van Schaik, A., Gediga, J., 2015. Simulation-based design for resource efficiency of metal production and recycling systems: Cases - copper production and recycling, e-waste (LED lamps) and nickel pig iron. Int. J. Life Cycle Assess. 20 (5), 671–693. https://doi.org/10.1007/s11367-015-0860-4.
Reuter, M.A., van Schaik, A., Gutzmer, J., Bartie, N., Abadías-Llamas, A., 2019. Challenges of the Circular Economy: A Material, Metallurgical, and Product Design Perspective. Annu. Rev. Mat. Res. 49 (1), 253–274. https://doi.org/10.1146/annurev-matsci-070218-010057.
Rinne, M., Aromaa-Stubb, R., Elomaa, H., Porvali, A., Lundström, M., 2024. Evaluation of hydrometallurgical black mass recycling with simulation-based life cycle assessment. Int. J. Life Cycle Assess. 29 (9), 1582–1597. https://doi.org/10.1007/s11367-024-02304-y.
Ruismäki, R., Rinne, T., Dańczak, A., Taskinen, P., Serna-Guerrero, R., Jokilaakso, A., 2020. Integrating Flotation and Pyrometallurgy for Recovering Graphite and Valuable Metals from Battery Scrap. Metals 10 (5), 680. https://doi.org/10.3390/met10050680.
Scheidema, M., Reuter, M., & Roine, A. (2016). Life Cycle Assessment of Metallurgical Processes Based on Physical Flowsheet Models_Scheidema et al. REWAS, 179–185. doi: 10.1007/978-3-319-48768-7_26.
Schenker, V., Oberschelp, C., Pfister, S., 2022. Regionalized life cycle assessment of present and future lithium production for Li-ion batteries. Resour. Conserv. Recycl. 187, 106611. https://doi.org/10.1016/j.resconrec.2022.106611.
Schwich, L., Schubert, T., Friedrich, B., 2021. Early-Stage Recovery of Lithium from Tailored Thermal Conditioned Black Mass Part I: Mobilizing Lithium via Supercritical CO2-Carbonation. Metals 11 (2), 177. https://doi.org/10.3390/met11020177.
Si, Z., Han, D., Xiang, J., 2021. Experimental investigation on the mechanical vapor recompression evaporation system coupled with multiple vacuum membrane distillation modules to treat industrial wastewater. Sep. Purif. Technol. 275, 119178. https://doi.org/10.1016/j.seppur.2021.119178.
Stallmeister, C., Friedrich, B., 2023. Influence of Flow-Gas Composition on Reaction Products of Thermally Treated NMC Battery Black Mass. Metals 13 (5), 923. https://doi.org/10.3390/met13050923.
Stallmeister, C., Mehl, N., Friedrich, B., 2025. Microwave thermal treatment of industrial NMC 622 lithium-ion battery shredder and its influence on reaction products compared to conventional pyrolysis. J. Environ. Manage. 377, 124616. https://doi.org/10.1016/j.jenvman.2025.124616.
Steubing, B., de Koning, D., Haas, A., Mutel, C.L., 2020. The Activity Browser — An open source LCA software building on top of the brightway framework. Software Impacts 3, 100012. https://doi.org/10.1016/j.simpa.2019.100012.
Swain, B., 2017. Recovery and recycling of lithium: A review. Sep. Purif. Technol. 172, 388–403. https://doi.org/10.1016/j.seppur.2016.08.031.
Toper. (2025). https://www.industrial-filterpress.com/sale-48318647-450x450mm-plate-hydraulic-compress-industrial-filter-press-function-of-solid-liquid-separation.html.
Träger, T., & Friedrich, B. (2016). Demonstrationsanlage für ein kostenneutrales, ressourceneffizientes Processing ausgedienter Li-Ion-Batterien der Elektromobilität - EcoBatRec: Förderkennzeichen 16EM1003.
Wang, H., Friedrich, B., 2015. Development of a Highly Efficient Hydrometallurgical Recycling Process for Automotive Li–Ion Batteries. Journal of Sustainable Metallurgy 1 (2), 168–178. https://doi.org/10.1007/s40831-015-0016-6.
Wang, K., Liu, S., Chen, L., Huang, Y., Sun, X., Chu, Q., Zhang, Y., 2025. Recycle of graphite and recovery of valuable metals from industrial-grade black mass of spent lithium-ion battery. Chinese Journal of Chemical Engineering. Advance online publication. https://doi.org/10.1016/j.cjche.2025.05.046.
Wang, Y., An, N., Wen, L., Wang, L., Jiang, X., Hou, F., Yin, Y., Liang, J., 2021. Recent progress on the recycling technology of Li-ion batteries. Journal of Energy Chemistry 55, 391–419. https://doi.org/10.1016/j.jechem.2020.05.008.
Wernet, G., Bauer, C., Steubing, B., Reinhard, J., Moreno-Ruiz, E., Weidema, B., 2016. The ecoinvent database version 3 (part I): overview and methodology. Int. J. Life Cycle Assess. 21 (9), 1218–1230. https://doi.org/10.1007/s11367-016-1087-8.
Xu, C., Dai, Q., Gaines, L., Hu, M., Tukker, A., Steubing, B., 2020. Future material demand for automotive lithium-based batteries. Communications Materials 1 (1). https://doi.org/10.1038/s43246-020-00095-x.
Zhang, C., He, N., Meng, X., Zhao, H., 2025. Advances in lithium and sodium separation techniques for brine lithium extraction processes. J. Environ. Chem. Eng. 13 (3), 116471. https://doi.org/10.1016/j.jece.2025.116471.
Zhang, L., Li, L., Rui, H., Shi, D., Peng, X., Ji, L., Song, X., 2020. Lithium recovery from effluent of spent lithium battery recycling process using solvent extraction. J. Hazard. Mater. 398, 122840. https://doi.org/10.1016/j.jhazmat.2020.122840.